THE COMPARISON OF STEEL FLOW IN SIX STRAND TUNDISH USING THREE DIFFERENT TYPES OF IMPACT PADS

[1]Peter DEMETER, [1]Branislav BUĽKO, [1]Róbert DZURŇÁK, [2]Ivan PRIESOL, [1]Slavomír HUBATKA, [1]Lukáš FOGARAŠ, [1]Jaroslav DEMETER, [1]Martina HRUBOVČÁKOVÁ

[1]Technical University of Košice, Faculty of Materials, Metallurgy and Recycling, Institute of Metallurgy, Košice, Slovakia, EU, peter.demeter@tuke.sk

[2]IPC REFRACTORIES s.r.o., Košice, Slovakia, ipriesol@ipc.sk

https://doi.org/10.37904/metal.2023.4623

Abstract

In this paper, the research of steel flow characteristics using three different shapes of impact pads in a 6-strands tundish is presented.

The key purpose of the research presented in this paper was to improve flow characteristics and steel temperature distribution across the whole tundish inner space with the aim of preventing erosion of the refractory lining in the upper section of the inflow area. Simulations were realized for various types and shapes of impact pads. The steel flow in the tundish was evaluated using vectors, contours, streamlines, RTD curves, and the values of minimum and maximum residence times.

The results indicated that the application of different shapes of impact pads may improve the flow characteristics in terms of homogenizing residence times for the individual outlets and adjusting the proportions of the mixing zones, which has a significant effect on thermal and chemical homogenization, possibility to refine steel, i.e. purify it from non-metallic inclusions and erosion of the tundish refractory lining.

Keywords: Tundish, numerical modelling, non-isothermal flows, CFD, impact pad

1. INTRODUCTION

A tundish is a main component of a continuous steel casting machine. It serves as a reservoir for molten metal when a ladle is replaced, and it is the last refractory-lined section where the quality of the casted steel can still be improved or degraded. Today, the tundish has multiple functions beyond just conducting liquid steel to individual outlets, reducing the effect of metal ferrostatic pressure on the melt level in a mold, and minimizing cast stream distribution. It is also used for deoxidation, micro-alloying, chemical and temperature homogenization of steel, and refining steel purity through interphase reactions at the steel-slag interface [1–4]. The tundish serves as an efficient continuous metallurgical reactor, with different zones for flow optimization, including the dead zone, the perfectly mixed zone, and the plug flow zone [4–6]. Multiple factors affect the optimization of tundish shape, including the number and spacing of steel outlets, the position of the ladle, casting velocity, cross-section of the continuously cast steel product, ladle turnover time, casting start-up, slag and skull removal, and the metal flow pattern.

2. CHARACTERISTICS OF IMPACT PADS

The primary objective of this research was to enhance the flow characteristics and steel temperature distribution throughout the entire tundish space to prevent erosion of the lining in the upper section of the inflow area. Various simulations were realised using different types of impact pads. The evaluation tools included vectors, contours, streamlines, RTD curves, and the values of minimum and maximum residence times to

assess the steel temperature distribution, increase the tundish refining ability to remove non-metallic inclusions, and reduce erosion of the refractory lining. The initial phase of the investigation used the "SPHERIC" impact pad, which was described in International Patent Application [7] and International Patent Classification [8]. The main hypothesis was to reduce the hydrodynamic drag of the impacting stream of molten steel by altering the shape of the impacted objects and the drag coefficient (C) applied in the equation for dimensional analysis of the resistive force F.

$$F = \frac{1}{2} C \cdot \rho \cdot S \cdot v \quad (1)$$

wherein:

C - coefficient of drag (-)

ρ - specific mass of fluid ($N \cdot m^{-3}$)

S - size of the reference area (planform area of the pad) (mm)

v - relative velocity of impinging stream ($m \cdot s^{-1}$)

Table 1 presents the C coefficient, a dimensionless parameter that can be considered mostly constant despite minor variations in velocity. When it comes to objects placed in a stream that's freely flowing, empirical data indicates that the drag coefficient for a square plate is 1.17 and for a convex hemisphere, it's 0.40 (as referenced in [9,10,11]). As described in [9], the suggested spherical pad has a square-shaped base and a hemispherical upper surface with a considerable diameter.

Table 1 The drag coefficient is determined by the shape of an object or its profile [11]

Shapes and profiles of Solids	Coefficient of drag – C
Circular plate	1.11
Square plate	1.05 to 1.27
Hollow hemisphere	1.35 to 1.40
Convex hemisphere	0.30 to 0.40

Since each tundish is distinct, there is no one universally appropriate shape for an impact pad. However, choosing an appropriate impact pad shape can have a significant impact on flow characteristics if the tundish shape is already determined. Thus, impact pads should be tailored to the specific structure, shape, and internal configuration of the tundish.

To achieve optimal flow and refining characteristics in modern tundish metallurgy, advanced tools such as mathematical simulations are utilized. These simulations employ numerical models to depict the behavior of a real system and can simulate various systems without interfering with the actual equipment. Mathematical simulations allow for precise monitoring of changes in boundary conditions and identification of various conditions to enhance equipment efficiency. Moreover, mathematical simulations can be applied in scenarios that cannot be investigated using real systems, presenting a notable advantage (as referenced in [12-14]).

After conducting preliminary simulations using ANSYS Discovery 2022 software from ANSYS, located in Canonsburg, PA, USA, a revised version of the "SPHERIC-PROTOTYPE" was created. The newly designed prototype features raised lateral walls to meet the specified requirements for the particular type of tundish.

The fundamental configuration of the tundish consisted of an impact pad named "KTHE/C" created by Zakłady Magnezytowe "ROPCZYCE" S.A. located at Postępu 15c Street, 02-676 Warsaw, Poland. The figures illustrate the key measurements of the impact pads tested: **Figure 1** shows the dimensions for "KTHE/C" (K Configuration), **Figure 2** for "SPHERIC-PROTOTYPE-A," (SP-A Configuration), and **Figure 3** for "SPHERIC-PROTOTYPE-B" (SP-B Configuration).

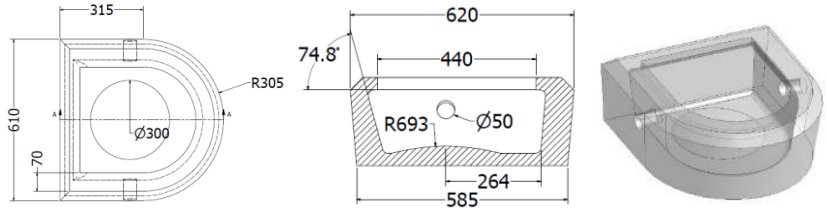

Figure 1 "KTHE/C"

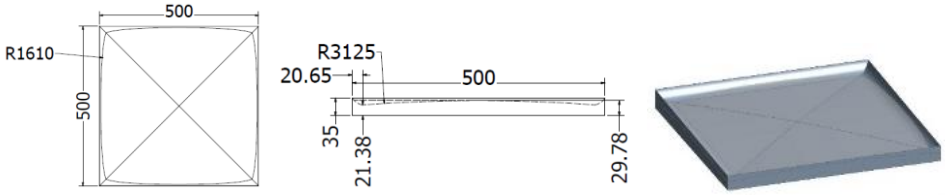

Figure 2 "SPHERIC-PROTOTYPE-A"

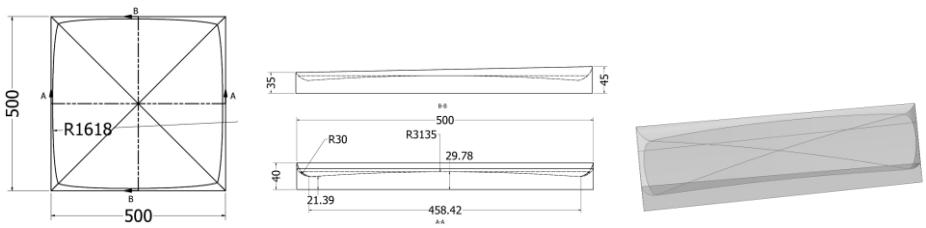

Figure 3 "SPHERIC-PROTOTYPE-B"

3. NUMERICAL MODELING

The study used CFD simulations realised in Ansys Fluent, a software developed by ANSYS, headquartered in Canonsburg, PA, USA. The calculations were realised using 3D models, and since turbulent flow is common in most real cases, a turbulent model was necessary. Specifically, the realizable k-epsilon model [15-17] was used in the calculation.

The Realizable $k-$epsilon model contains a modified turbulent viscosity formulation and a modified transport equation for ε. The Realizable model brings improvements for flows with large curvature of the streams, eddies and rotations [16-19].

A particle transport model was used to identify the residence time.

To model the flow accurately, it was crucial to create a representation of the tundish's internal volume, which measures 5.6989 m³. The model was based on the basic dimensions of the tundish, including the "SPHERIC" impact pad, as depicted in **Figure 4**.

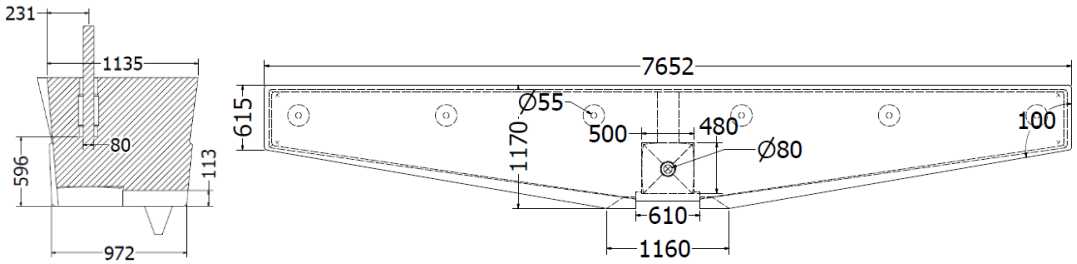

Figure 4 A technical drawing of the analysed 6-strand tundish

A polyhedral computational mesh, consisting of 1,404,422 elements was created. Skewness and orthogonality criteria were used to evaluate the mesh's quality, yielding a skewness value of 0.32 and an orthogonality value of 0.99. The turbulent nature of the flow under analysis required the application of a boundary layer during mesh creation. Additionally, inflow and outflow zones, as well as the walls of the tundish model, were defined to allow for subsequent specification of initial and boundary conditions.

Table 2 contains a list of the boundary and baseline conditions values used for CFD simulations.

Table 2 Parameters and boundary conditions used in modelling

Parameter	Value
Model	
Diameter of ladle shroud (mm)	80
Depth of molten steel (mm)	930
Material	
Inlet temperature (K)	1,823
Density of molten steel (kg·m^{-3})	7,020
Viscosity of molten steel (kg·m^{-1}·s^{-1})	0.0067
Specific heat (J·kg^{-1}·K^{-1})	750
Thermal conductivity (w·m^{-1}·K^{-1})	41
Heat flux (kw·m^{-2})	15
Inlet	
Mass flow rate (kg·s^{-1})	11.36
Turbulent intensity (%)	3.48
Hydraulic diameter (m)	0.08
Outlet	
Pressure outlet	0
Turbulent intensity (%)	3.64
Hydraulic diameter (m)	0.055
Walls	
Walls (flow)	No slip
Thermal conditions (K)	1,777
Wall (heat loss) (kW·m^{-2})	2.5
Surface (heat loss) (kW·m^{-2})	15
Tracer	
Injection time (s)	10

4. EVALUATION AND DISCUSSION

To evaluate the CFD simulations, flow patterns were observed through various means such as contours, vectors, streamlines and temperature distribution of molten steel in specific planes for both configurations. In addition, measurements of steel distribution over time were compared using RTD curves and residence time values. The analysis also focused on individual zones that represent the actual reactors within the interconnected flow zones, including the plug flow zone, perfectly mixed zone and dead zone.

In three planes (**Figure 5**), a visual assessment of flow characteristics was performed utilizing vectors, contours, and streamlines.

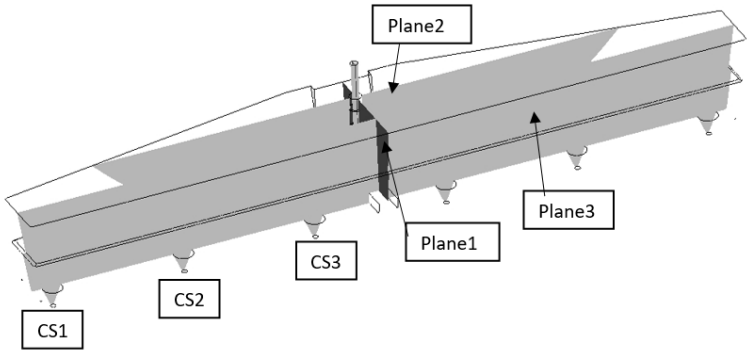

Figure 5 Analysed planes and outlet designations in the simulation model

The flow of the injected tracer was depicted by visually observing contours. Observing the individual configurations made it possible to notice flow differences depending on the impact pad used. With K Configuration, the contours indicated a plug flow. This type of flow may cause that the metal surface is uncovered due to the slag “red eye” phenomena.

In contrast, the SP-A Configuration displayed a flow change towards the upper front portion of the tundish. This flow pattern improves the distribution of metal throughout the tundish, resulting in better utilization of its volume. On the other hand, the SP-B Configuration redirected the flow partly across the space and partly towards the inflowing steel through the ladle shroud.

Observing the flow of the tracer indicated the need to prevent a short-circuit flow, particularly at the CS3 outlet.

By observing the flow patterns, it was evident that with the K Configuration, the tracer only flowed in the upper section of the inflow area. This occurrence has the potential to result in the washing out and erosion in the slag line area.

After analysing the vectors using the K Configuration as a reference, it can be inferred that the upper central part of the tundish near the ladle shear is the most stressed portion of the lining. On the other hand, with the SP-A and SP-B Configurations, the rear part of the tundish, specifically the area behind the ladle shroud, experienced the most mechanical stress. Fortunately, this area is not at risk since it is already equipped with a monolithic reinforced plate.

Visualizing the streamlines of the tundish enabled tracking of the monitored particle's trajectory until it reached an outlet. In comparison to the reference configuration (K Configuration), where the streamlines initially flowed towards the central outlets, the streamlines in the SP-A Configuration first flowed towards the rear section of the inflow area and then towards the outlets, resulting in extended residence times for CS3. With the SP-B Configuration, the flow was uniformly distributed in all directions in the inflow area.

Comparison of temperature distribution between the SP-A and reference K Configurations indicated that the highest temperatures were present in the inflow area of the tundish, implying better mixing due to the impact of the “SP-A” and “SP-B” impact pads. Another observation was that the steel temperatures were more evenly distributed in the areas farther from the impact pad. In contrast, the use of the reference “KTHE/C” impact pad led to the highest temperatures in the upper rear and front inflow areas, particularly near the ladle shroud, suggesting less thorough mixing of the inflowing steel with the entire steel volume inside the tundish.

The flow characteristics of the symmetrical tundish were assessed by analysing the RTD curves and determining the minimum and maximum residence times for the CS1 (located farthest from the inlet), CS2, and CS3 outlets (**Figure 5**).

Table 3 presents the minimum and maximum residence times for the analysed configurations, which were determined using the C-curves at each individual outlet. These values were compared with respect to the reference K Configuration.

Table 3 Calculation parameters of RTD and flow velocity volume proportions

Resulting min. and max. residence times							$\frac{V_d}{V}$	$\frac{V_p}{V}$	$\frac{V_m}{V}$
	T_{min} (s)			T_{max} (s)			(%)		
Configuration	CS1	CS2	CS3	CS1	CS2	CS3			
K	168	56	28	387	103	37	19.9	25.8	54.3
SP-A	80	41	33	180	60	65	31.7	15.2	53.1
SP-B	65.2	39.5	43.3	180	50	73.9	19.9	9.8	70.3

The minimum residence time values for the outlet CS1 show that there is a 52% decrease in T_{min} when comparing the K Configuration to the SP-A Configuration. Similarly, there was a decrease of 26.8% at CS2, but an increase of 17.8% at CS3. This trend has a significant impact on the tundish refining capacity.

Regarding the computed dead volumes in the tundish, it was observed that the SP-A Configuration had a higher dead volume compared to the K Configuration. Conversely, there was a reduction in the plug volume. The mixed zone showed similar results for the SP-A Configuration but exhibited an increase for the SP-B Configuration.

5. CONCLUSION

The observation of flow characteristics based on vectors facilitated preventing erosion of the upper section of the inflow area of the tundish caused by inflowing molten steel. The flow was redirected towards the rear section of the tundish, outside the inflow area. This led to changes in flow characteristics within the tundish space, resulting in homogenized residence times at individual outlets calculated based on the RTD curves.

Visual observation revealed that the temperature distribution of molten steel was more evenly distributed throughout the entire tundish space. This was achieved by extending the temperature field in the inflow area with the "SPHERIC-PROTOTYPE-A" and "SPHERIC-PROTOTYPE-B" impact pads. The results of CFD simulations for these impact pads indicate that they can eliminate areas with lining erosion and achieve homogenized residence times at individual outlets.

ACKNOWLEDGEMENTS

This research work was performed under the grant project No. 1/0212/21 and was financially supported by VEGA ME SR and SAS, and project APVV-21-0396 was financially supported by APVV.

REFERENCES

[1] XU, P., ZHOU, Y-Z., CHEN, D-F., LONG, M-J., DUAN, H-M. Optimization of submerged entry nozzle parameters for ultra-high casting speed continuous casting mold of billet. *J. Iron Steel Res. Int.* 2022, vol. 29, pp. 44–52. Available from: https://doi.org/10.1007/s42243-021-00701-3.

[2] WARZECHA, M., MERDER, T., WARZECHA, P., HUTNY, A.M. Hydrodynamic Conditions of Flow in the Tundish Depending on Selected Technological Parameters for Different Steel Groups. *Arch. Metall. Mater*. 2019, vol. 64, no. 1, pp. 65-70. Available from: https://doi.org/10.24425/amm.2019.126219.

[3] GUTHRIE, R. I. L., ISAC, M. M. Continuous Casting Practices for Steel: Past, Present and Future. *Metals.* 2022, vol. 12, no.5, pp. 862. Available from: https://doi.org/10.3390/met12050862.

[4] SOWA, L. Effect of Steel Flow Control Devices on Flow and Temperature Field in the Tundish of Continuous Casting Machine. *Archives of Metallurgy and Materials*. 2015, vol. 60, no. 2. Available from: https://doi.org/10.1515/amm-2015-0216.

[5] PIEPRZYCA, J., MERDER, T., LIPINSKI, J., LASKAWIEC, D. Physical model of CCM for research in isothermal and non-isothermal conditions. *Hutnik-Wiadomości hutnicze*. 2010, vol. 10, pp. 567-571.

[6] GRYC, K., MICHALEK, K., STŘASÁK, P. Optimizing the internal configuration of the tundish to achieve temperature homogeneity of continuously cast steel, In: *Metal 2007*. Ostrava: Tanger, 2007. pp. 38-38. ISBN 978-80-86840-33-8.

[7] PRIESOL, I. A Method of Molten Metal Casting Utilizing an Impact Pad in the Tundish. International Patent Application No. PCT/IB2016/056207, 2016.

[8] PRIESOL, I. Spôsob Liatia Roztaveného Kovu s Využitím Dopadovej Dosky v Tundish. International Patent Classification: B22D 11/10 B22D 41/00, Application No. 109-2016, 2016, B22D 11/00 B22D 41/00, Application No. 89-2016, 2016.

[9] HOERNER, S.F. Fluid Dynamic Drag: *Practical Information on Aerodynamic Drag and Hydrodynamic Resistance.* Hoerner Fluid Dynamics: Bakersfield, CA, USA, 1965.

[10] KIREŠ M, LABUDA J. Mechanics of liquids and gases. [online]. 2018 [viewed: 2018-09-17]. Available from: http://physedu.science.upjs.sk/kvapaliny/obtekanie.htm.

[11] BUĽKO, B., PRIESOL, I., DEMETER, P., GAŠPAROVIČ, P., BARICOVÁ, D., HRUBOVČÁKOVÁ, M. The Geometric Modification of Impact Point in Tundish. *Metals.* 2018, vol. 8, no. 11, pp. 944. Available from: https://doi.org/10.3390/met8110944.

[12] LIU, J., ZHOU, P., ZUO, X., WU, D., WU, D. Optimization of the Liquid Steel Flow Behavior in the Tundish through Water Model Experiment, Numerical Simulation and Industrial Trial. *Metals.* 2022, vol. 12, pp. 1480. Available from: https://doi.org/10.3390/met12091480.

[13] TKADLEČKOVÁ, M., WALEK, J., MICHALEK, K., HUCZALA, T. Numerical Analysis of RTD Curves and Inclusions Removal in a Multi-Strand Asymmetric Tundish with Different Configuration of Impact Pad. *Metals*. 2020, vol. 10, pp. 849. Available from: https://doi.org/10.3390/met10070849.

[14] YANG, B., LEI, H., XU, Y., LIU, K., HAN, P. Numerical Investigation of Flow Characteristics of Molten Steel in the Tundish with Channel Induction Heating. Metals. 2021, vol. 11, pp. 1937. Available from: https://doi.org/10.3390/met11121937.

[15] VLČEK, P. Modelování turbulentního proudění. [online]. 2013 [viewed: 2020-03-31] Available from: http://chps.fsid.cvut.cz/pt/2013/pdf/3509.pdf.

[16] SHENG, D.-Y. Design Optimization of a Single-Strand Tundish Based on CFD-Taguchi-Grey Relational Analysis Combined Method. *Metals.* 2020, vol. 10, pp. 1539. Available from: https://doi.org/10.3390/met10111539.

[17] TKADLECKOVA, M., VALEK, L., SOCHA, L., SATERNUS, M., PIEPRZYCA, J., MERDER, T., MICHALEK, K., KOVAC, M. Study of solidification of continuously cast steel round billets using numerical modelling. *Archives of metallurgy and materials*. 2016, vol. 61, no. 1, pp. 221-226. Available from: https://doi.org/10.1515/amm-2016-0041.

[18] MICHALEK, K., TKADLECKOVA, M., SOCHA, L., GRYC, K., SATERNUS, M., PIEPRZYCA, J., MERDER, T. Physical Modelling of Degassing Process by Blowing of Inert Gas, *Archives of metallurgy and materials*. 2018, vol. 63, no. 2, pp. 987-992. Available from: https://doi.org/10.24425/122432.

[19] TKADLECKOVA, M., MICHALEK, K., STROUHALOVA, M., SVIZELOVA, J., SATERNUS, M., PIEPRZYCA, J., MERDER, T. Evaluation of Approaches of Numerical Modelling of Solidification of Continuously Cast Steel Billets, *Archives of metallurgy and materials*. 2018, vol. 63, no. 2, pp. 1003-1008. Available from: https://doi.org/10.24425/122435.